Mon. Not. R. Astron. Soc. **000**, 000–000 (0000) Printed 28 April 2010 (MN LATEX style file v2.2)

The dynamics of pulsar glitches: Contrasting phenomenology with numerical evolutions

T. Sidery[1], A. Passamonti[2] and N. Andersson[2]

[1] *FENS, Sabanci University, Orhanli, 34956 Istanbul, Turkey*
[2] *School of Mathematics, University of Southampton, Southampton SO17 1BJ, United Kingdom*

arXiv:0910.3918v2 [astro-ph.HE] 27 Apr 2010

28 April 2010

ABSTRACT

In this paper we consider a simple two-fluid model for pulsar glitches. We derive the basic equations that govern the spin evolution of the system from two-fluid hydrodynamics, accounting for the vortex mediated mutual friction force that determines the glitch rise. This leads to a simple "bulk" model that can be used to describe the main properties of a glitch event resulting from vortex unpinning. In order to model the long term relaxation following the glitch our model would require additional assumptions regarding the repinning of vortices, an issue that we only touch upon briefly. Instead, we focus on comparing the phenomenological model to results obtained from time-evolutions of the linearised two-fluid equations, i.e. a "hydrodynamic" model for glitches. This allows us to study, for the first time, dynamics that was "averaged" in the bulk model, i.e. consider the various neutron star oscillation modes that are excited during a glitch. The hydro-results are of some relevance for efforts to detect gravitational waves from glitching pulsars, although the conclusions drawn from our rather simple model are pessimistic as far as the detectability of these events is concerned.

Key words: methods: numerical – stars: neutron – stars: oscillation – star:rotation – pulsars:general – gravitational waves

1 INTRODUCTION

Neutron stars provide excellent testbeds for extreme physics theory. Since their core density reaches beyond anything we can produce in the laboratory, observations of such compact remnants may provide unique constraints on models for supranuclear physics (Lattimer & Prakash 2004). In order to infer useful information from astrophysical observations we need to construct realistic models with the power to predict the evolution of individual systems (at least to some extent). This is a serious challenge for the modelling community. Even a moderately reasonable neutron star model should account for the presence of different exotic states of matter. From nuclear physics and Bardeen-Cooper-Schrieffer (BCS) theory we expect the outer neutron star core to consist of superfluid neutrons, superconducting protons, free electrons and muons. Deeper into the core more exotic phases of matter, like superfluid hyperons and/or deconfined quarks exhibiting colour-flavour-locked superconductivity, are likely to be present. Meanwhile, a relatively thin (1 km or so) crust surrounds the fluid core. In the crust, matter changes from a soup of nucleons in the interior to an elastic nuclear lattice of heavy iron near the surface. In the inner part of the crust (beyond neutron drip) free neutrons are expected to be superfluid.

An important question concerns whether differences in internal structure can be deduced from observations. This is obviously problematic since most of the data collected for these stars originate from the star's surface, atmosphere or magnetosphere. Having said that, there are phenomena that involve bulk dynamics and which should depend on the internal composition. Examples of such phenomena are the radio pulsar glitches (Lyne et al. 2000) and the quasi-periodic oscillations observed in the X-rays from magnetar flares, see for example Watts & Strohmayer (2007). The long relaxation time associated with glitches is seen as indirect evidence for neutron star superfluidity (Anderson & Itoh 1975; Ruderman 1976; Alpar et al. 1981), and recent considerations of the crust oscillations which are thought to be the origin of the observed magnetar oscillations suggest that these may be affected by the presence of a crust superfluid as well (Andersson et al. 2009).

In this paper we discuss basic models for pulsar glitches. We focus on the glitch event itself rather than the subsequent long term relaxation. We consider the implications of the standard two-fluid model from two different points of view. First of all, we derive the simple equations that govern the bulk evolution of the system from two-fluid hydrodynamics, accounting for the vortex mediated mutual friction force. This leads to a basic model that can be used to describe a glitch rise resulting from global vortex unpinning, be it in the crust (Link & Epstein 1996; Melatos et al. 2008; Warszawski & Melatos 2008; Melatos & Warszawski 2009) or in the core (Link 2003)[1]. The results demonstrate that the model requires additional assumptions regarding the repinning of vortices in order to model the long-term evolution. This is as expected (Alpar et al. 1984). Secondly, we use time-evolution of the linearised two-fluid equations as a "hydrodynamic" model for the glitch event. This allows us to consider dynamics that was "averaged" in the bulk model. In particular, we consider the various neutron star oscillation modes that are excited during the glitch. In principle, the obtained results could be of relevance for efforts to detect gravitational waves from glitching pulsars. Having said that, our estimates suggest that the gravitational-wave signals associated with the impulsive events that we consider here are very weak.

2 BULK PROPERTIES

We want to consider the simplest viable model for large pulsar glitches. The angular momentum of any superfluid component is determined by the density and configuration of vortices threading the fluid. If the vortices are fixed (pinned), there can be no angular momentum exchange between the superfluid and other components in the star. Assuming a scenario of catastrophic unpinning it is straightforward to formulate a simple glitch model. One can simply assume that the system has two components, with different moments of inertia and spin-rates. Adding the assumption that vortex pinning allows a lag in the rotation between the observed component (e.g. the crust) and the other component (the interior superfluid) and that the pinning breaks once a critical lag is reached, one arrives at a phenomenological glitch model. In order to effect the rapid transfer of angular momentum that leads to the observed spin-change in the crust, one would typically assume that the rotation lag relaxes on some timescale. The standard model assumes that this relaxation is due to the mutual friction acting on the superfluid vortices (Alpar et al. 1984; Mendell 1991; Andersson et al. 2006).

While such a phenomenological model is useful, its scope is limited. Ultimately, a detailed description will require a hydrodynamics analysis. In particular, if we want to understand the reason for the sudden vortex unpinning (likely due to an instability, see Andersson et al. (2003); Glampedakis & Andersson (2009) for recent ideas) and possible neutron star oscillations excited by the event. Developing a detailed hydrodynamics model is a severe challenge given the many uncertainties in the relevant physics, but we can make some progress by making contact between the general two-fluid hydrodynamics framework and the phenomenological bulk dynamics description. As a suitable starting point, we will show how the bulk model can be obtained from hydrodynamics. This is instructive since it provides insight into the validity of the model, and also gives us a better idea of the origin of the different parameters (like the global spin-up time). Moreover, we will be able to make direct comparisons with hydrodynamics results.

2.1 Single fluid

It is useful to begin by outlining the analysis of a single fluid body. In that case, we have a velocity field v_i which evolves according to the Euler equations;

$$\mathcal{E}_i = \left(\frac{\partial}{\partial t} + v^j \nabla_j\right) v_i + \nabla_i \left(\tilde{\mu} + \phi\right) = 0\,, \tag{1}$$

where ϕ is the gravitational potential and $\tilde{\mu} = \mu/m$ is the chemical potential divided by the particle mass. In addition, we have the continuity equation

$$\frac{\partial \rho}{\partial t} + \nabla_i \left(\rho v^i\right) = 0\,, \tag{2}$$

and the Poisson equation

$$\nabla^2 \phi = 4\pi G \rho\,. \tag{3}$$

Note that we use a coordinate basis to represent vector quantities throughout this paper. In other words, we distinguish between co- and contravariant quantities, using the flat space metric g_{ij} to relate them. That is, we have $v_i = g_{ij} v^j$. We also

[1] In reality, our model is somewhat unrealistic for both crust and core superfluids. In the former case we have not accounted for the crust elasticity, while in the latter case we are ignoring the expected interaction between neutron vortices and proton fluxtubes. These effects may have a decisive impact on glitch dynamics. Nevertheless, the present work is state-of-the-art in this area, and we expect to add the relevant features to the hydrodynamical model in future work.

make use of the Einstein summation convention for repeated indices. Finally, we have assumed that the internal energy E depends only on the number density n, i.e. that the fluid is a barotrope. Then

$$\mu = \frac{dE}{dn}\,, \tag{4}$$

and the pressure P of the fluid is defined (in the usual way) by

$$dP = nd\mu\,. \tag{5}$$

Viscosity terms have been omitted in anticipation of applying the solid body approximation, which we do now. Assuming uniform rotation the fluid velocity can be written

$$v_i = \epsilon_{ijk}\Omega^j x^k = \Omega\varpi\varphi_i\,, \tag{6}$$

where we take $\Omega = \Omega(t)$, ϖ is the cylindrical distance from the rotation (z) axis and φ_i is a unit vector in the direction of the flow. By assuming axi-symmetry it follows that

$$v^j\nabla_j v_i = 0\,, \tag{7}$$

$$v^j\nabla_j(\tilde{\mu}+\phi) = 0\,. \tag{8}$$

We will now derive the conservation of angular momentum and energy from the above equations. Contracting (1) with ρv_i and integrating over a fixed volume V gives

$$\frac{\partial E}{\partial t} = \int \rho v^j \frac{\partial v_j}{\partial t} dV = \frac{\partial}{\partial t}\left(\frac{1}{2}\int \rho v^2 dV\right) = 0\,. \tag{9}$$

This shows that the kinetic energy is conserved. Adding the assumption that the fluid is in solid body rotation we see that

$$v^2 = \Omega_j\Omega^k\left(\delta^j_k x^2 - x^j x_k\right)\,, \tag{10}$$

where $x^2 = g_{ij}x^i x^j = x^j x_j$. From this we define the moment of inertia as

$$I^i_l = \int \rho\left(\delta^i_l x^2 - x^i x_l\right) dV\,. \tag{11}$$

We can use (10) and (11) to rewrite the change in kinetic energy equation (9) as

$$\frac{\partial E}{\partial t} = \frac{1}{2}\frac{\partial}{\partial t}\left(I^i_l\Omega_i\Omega^l\right) = 0\,. \tag{12}$$

Let us now consider the z component of the angular momentum. Assuming that the chemical and gravitational potential only depend on the (spherical) radial position, i.e. assuming slow rotation, then

$$\epsilon_{ijk}x^j\nabla^k\left(\tilde{\mu}+\phi\right) = 0 \quad \text{for} \quad i = z\,. \tag{13}$$

Contracting $\mathcal{E}_i$ with $\rho\epsilon_{ijk}x^j$ and integrating gives

$$\begin{aligned}\frac{\partial J_i}{\partial t} &= \int \rho\epsilon_{ijk}x^j\mathcal{E}^k dV \\ &= \frac{\partial}{\partial t}\left[\int \rho\Omega_j\left(\delta^j_i x^2 - x_i x^j\right) dV\right] = \frac{\partial}{\partial t}\left(I^j_i\Omega_j\right) = 0 \quad \text{for} \quad i = z\,.\end{aligned} \tag{14}$$

We see that, for cylindrical polar coordinates with $\Omega^i = (0,0,\Omega)$ and $I^z_z = I$ we get the standard results

$$E = \frac{1}{2}I\Omega^2 \quad \text{and} \quad J^z = I\Omega\,. \tag{15}$$

Both these quantities are conserved.

2.2 Two-fluid model

We now consider a two constituent stellar model. Our particular interest concerns two effects, the entrainment and the mutual friction between the components. In order to simplify the initial analysis, we first ignore the mutual friction.

Our formulation for multi-fluid hydrodynamics in Newtonian gravity derives from the work by Prix (2004), see also Andersson & Comer (2006). The analysis is based on a variational principle, where the action is minimised by varying the fluid flow lines. Key in this analysis is the allowance that the internal energy may depend on the velocity difference between the two constituents, $w^{\rm np}_i = v^{\rm n}_i - v^{\rm p}_i$, such that

$$dE = \frac{\partial E}{\partial n_{\rm n}}dn_{\rm n} + \frac{\partial E}{\partial n_{\rm p}}dn_{\rm p} + \frac{\partial E}{\partial w^2_{\rm np}}dw^2_{\rm np} = \mu_{\rm n}dn_{\rm n} + \mu_{\rm p}dn_{\rm p} + \alpha dw^2_{\rm np}\,. \tag{16}$$

Here, the constituent indices n and p denote the neutron and "proton" (incorporating also electrons and muons in the usual way) components, respectively. An important consequence is that the conjugate momentum density for each constituent is modified so that

$$p^{\rm x}_i = \rho_{\rm x}\left[v^{\rm x}_i + \varepsilon_{\rm x}\left(v^{\rm y}_i - v^{\rm x}_i\right)\right]\,, \tag{17}$$

where x and y is either n or p, with x $\neq$ y. In this relation the entrainment is represented by the parameter $\varepsilon_{\rm x}$. This is a non-dissipative effect, in the neutron star case due to the strong interaction between neutrons and protons, which leads to the momentum no longer being aligned with the individual components velocity. We refer the read to Prix et al. (2004); Carter et al. (2005); Gusakov & Haensel (2005); Chamel & Carter (2006) for discussions of the role of entrainment in neutron star dynamics. Note that,

$$\varepsilon_{\rm x}\rho_{\rm x} = \varepsilon_{\rm y}\rho_{\rm y} = 2\alpha\,. \tag{18}$$

We now have a set of Euler equations for each constituent. These equations can be written

$$\mathcal{E}^{\rm x}_i = \left(\frac{\partial}{\partial t} + v^j_{\rm x}\nabla_j\right)(v^{\rm x}_i + \varepsilon_{\rm x} w^{\rm yx}_i) + \nabla_i\left(\phi + \tilde{\mu}_{\rm x}\right) + \varepsilon_{\rm x} w^{\rm yx}_j \nabla_i v^j_{\rm x} = 0\,. \tag{19}$$

In addition, we have one continuity equation for each component and the Poisson equation for ϕ is now sourced by the total mass density $\rho = \rho_{\rm n} + \rho_{\rm p}$. Following the analysis in the previous section, we want to derive the equations that represent the global conservation of energy and angular momentum. In doing this we will, for simplicity, assume that the velocity fields of the constituents are those of rotating solid bodies. We also assume that the two components rotate around the same axis, i.e. we ignore any precessional motion. This means that we can write

$$v^i_{\rm x} = \Omega_{\rm x}\varpi\varphi^i \quad \text{and} \quad w^i_{\rm yx} = v^i_{\rm y} - v^i_{\rm x} = (\Omega_{\rm y} - \Omega_{\rm x})\,\varpi\varphi^i\,. \tag{20}$$

As we are assuming solid body rotation, $\Omega_{\rm x}$ is not a function of position. Moreover, the axial symmetry of the system implies that

$$v^j_{\rm x}\nabla_j v^{\rm x}_i = 0\,, \tag{21}$$

$$v^j_{\rm x}\nabla_j\left(\phi + \tilde{\mu}_{\rm x}\right) = 0\,. \tag{22}$$

We continue to follow the method used in the single fluid case, contract $\mathcal{E}^{\rm x}_i$ with $\rho_{\rm x} v^{\rm x}_i$ and integrate over a fixed volume to find the global change in energy of each constituent. This leads to

$$\frac{\partial E_{\rm x}}{\partial t} = \int \rho_{\rm x} v^i_{\rm x}\mathcal{E}^{\rm x}_i dV = \frac{1}{2}\int\left[(\rho_{\rm x} - 2\alpha)\frac{\partial}{\partial t}v^2_{\rm x} + 4\alpha v^j_{\rm x}\frac{\partial v^{\rm y}_j}{\partial t}\right]dV = 0\,. \tag{23}$$

We obtain the final result for the total change in energy by adding the expressions for the two components,

$$\frac{\partial E}{\partial t} = \frac{\partial E_{\rm n}}{\partial t} + \frac{\partial E_{\rm p}}{\partial t} = \frac{1}{2}\frac{\partial}{\partial t}\left\{\int\left[\rho_{\rm n}v^2_{\rm n} + \rho_{\rm p}v^2_{\rm p} - 4\alpha w^2_{\rm np}\right]dV\right\} = 0\,. \tag{24}$$

This result shows how the entrainment affects the conserved energy, cf. Carter & Chamel (2004) for a detailed discussion, and agrees perfectly with the modified "kinetic energy" used by Mendell (1991).

In the particular case of (aligned) solid-body rotation, with $\Omega^{\rm x}_i$ aligned with the z-axis, we have

$$\frac{\partial E}{\partial t} = \frac{\partial}{\partial t}\left\{\frac{1}{2}I_{\rm n}\Omega_{\rm n}\left[\Omega_{\rm n} + \varepsilon_{\rm n}\left(\Omega_{\rm p} - \Omega_{\rm n}\right)\right] + \frac{1}{2}I_{\rm p}\Omega_{\rm p}\left[\Omega_{\rm p} + \varepsilon_{\rm p}\left(\Omega_{\rm n} - \Omega_{\rm p}\right)\right]\right\} = 0\,. \tag{25}$$

Here we have defined the constituent moment of inertia as

$$I_{{\rm x}i}{}^j = \int \rho_{\rm x}\left(\delta^j_i x^2 - x_i x^j\right)dV\,, \tag{26}$$

and $I_{\rm x} = I_{{\rm x}z}{}^z$. Similarly, we can calculate the total change in angular momentum. To do this we note that

$$\epsilon_{ijk}x^j v^l_{\rm x}\nabla^k v^{\rm x}_l = \epsilon_{ijk}x^j x^k\Omega^2_{\rm x} - \epsilon_{ijk}x^j\Omega^k_{\rm x}x_l\Omega^l_{\rm x} = 0 \quad \text{for} \quad i = z\,, \tag{27}$$

as $\Omega^{\rm x}_i$ is parallel to the z-axis. Contracting $\mathcal{E}^{\rm x}_i$ with $\rho_x\epsilon_{ijk}x^j$ and integrating over the volume V we arrive at

$$\begin{aligned}\frac{\partial J^{\rm x}_i}{\partial t} &= \int \rho_{\rm x}\epsilon_{ijk}x^j\mathcal{E}^k dV \\ &= \int \rho_{\rm x}\epsilon_{ijk}x^j\left[(1-\varepsilon_{\rm x})\frac{\partial v^k_{\rm x}}{\partial t} + \varepsilon_{\rm x}\frac{\partial v^k_{\rm y}}{\partial t}\right]dV = 0 \quad \text{for} \quad i = z\,.\end{aligned} \tag{28}$$

This can be rewritten as

$$\frac{\partial J^{\rm x}_i}{\partial t} = \frac{\partial}{\partial t}\left\{I_{{\rm x}i}{}^j\left[\Omega^{\rm x}_j + \varepsilon_{\rm x}\left(\Omega^{\rm y}_j - \Omega^{\rm x}_j\right)\right]\right\} = 0 \quad \text{for} \quad i = z\,, \tag{29}$$

from which it follows that the total change in angular momentum is given by

$$\frac{\partial J_z}{\partial t} = \frac{\partial}{\partial t}\left(I_{\rm n}\Omega_{\rm n} + I_{\rm p}\Omega_{\rm p}\right) = 0\,. \tag{30}$$

Hence, the total angular momentum is conserved. This is obviously not surprising. The non-trivial result concerns how the entrainment affects the evolution of the individual components. This will be important later.

3 A SIMPLE SPIN-DOWN MODEL

We are not yet in a position where we can model glitches. To do this, even in the most basic fashion, we need to account for the coupling due to mutual friction. However, before we discuss that problem it is interesting to consider how the conservation equations that we have obtained can be used to model the rotational evolution of the system. The main purpose of doing this is to understand how the entrainment enters the problem. As we will see, the result can be quite surprising.

Equation (29) shows that the angular momentum of each constituent is conserved. In a neutron star we would expect the protons to be locked to the magnetic field and the crust. Hence, they should be spun down due to a magnetic torque $j_i^{\rm em}$. We can include this torque in the equations by breaking the conservation of the proton angular momentum, so that

$$j_i^{\rm p} = -j_i^{\rm em}\,, \tag{31}$$

(from now on we will often represent time derivatives by dots). To be specific, we assume that the magnetic torque is related to the angular velocity of the protons by

$$\dot{J}_{\rm em} = \mathcal{A} I_{\rm p} \Omega_{\rm p}^3\,. \tag{32}$$

This is in accord with the standard magnetic dipole model. We will also assume that the constituent moments of inertia are constant. Noting that $I_{\rm n}\varepsilon_{\rm n} = I_{\rm p}\varepsilon_{\rm p}$ and defining $\varepsilon = \varepsilon_{\rm p}$ equation (29) leads to

$$I_{\rm n}\dot{\Omega}_{\rm n} + I_{\rm p}\varepsilon\left(\dot{\Omega}_{\rm p} - \dot{\Omega}_{\rm n}\right) = 0\,, \tag{33}$$

$$I_{\rm p}\dot{\Omega}_{\rm p} + I_{\rm p}\varepsilon\left(\dot{\Omega}_{\rm n} - \dot{\Omega}_{\rm p}\right) = -\mathcal{A} I_{\rm p}\Omega_{\rm p}^3\,. \tag{34}$$

Defining $\tilde{I} = I_{\rm p}/I_{\rm n}$ equation (33) gives

$$\dot{\Omega}_{\rm n} = -\frac{\varepsilon\tilde{I}}{1-\varepsilon\tilde{I}}\dot{\Omega}_{\rm p}\,. \tag{35}$$

Substituting this into equation (34) we get

$$\bar{I}\dot{\Omega}_{\rm p} \equiv \left(1 - \frac{\varepsilon}{1-\varepsilon\tilde{I}}\right)\dot{\Omega}_{\rm p} = -\mathcal{A}\Omega_{\rm p}^3\,. \tag{36}$$

This is a separable equation so we can integrate to get

$$\int_{\Omega_0}^{\Omega_{\rm p}} \frac{d\Omega_{\rm p}}{\Omega_{\rm p}^3} = -\frac{\mathcal{A}}{\bar{I}}\int_{t_0}^{t} dt\,, \tag{37}$$

where Ω_0 is $\Omega_{\rm p}$ at time t_0. Setting $t_0 = 0$ we find the solution

$$\Omega_{\rm p} = \Omega_0\left(1 + \frac{2\mathcal{A}\Omega_0^2 t}{\bar{I}}\right)^{-1/2}\,. \tag{38}$$

As we expect the evolution to be slow, the second term in the bracket is small and we can expand to get

$$\Omega_{\rm p} \approx \Omega_0\left(1 - \frac{\mathcal{A}\Omega_0^2 t}{\bar{I}}\right)\,. \tag{39}$$

From this we can find the characteristic evolution timescale τ for the crust (the protons). Ignoring entrainment we have

$$\tau = \frac{1}{\mathcal{A}\Omega_0^2}\,. \tag{40}$$

$\mathcal{A}$ can be calculated from the standard magnetic dipole model (Shapiro & Teukolsky 1983). Modifying the result so that the torque acts on the proton fluid rather than the whole star we find

$$\mathcal{A} = \frac{B_{\rm p}^2 R^6 \sin^2\theta}{6c^3 I_{\rm p}}\,, \tag{41}$$

where $B_{\rm p}$ is the strength of the magnetic dipole with axis at an angle θ to the rotation axis, R is the radius of the star and c is the speed of light. As $I_{\rm p} \ll I_{\rm n} \approx I$ (typically), we can use

$$I_{\rm p} \approx \frac{I_{\rm p}}{I_{\rm n}} I \approx \frac{I_{\rm p}}{I_{\rm n}}\frac{2MR^2}{5}\,, \tag{42}$$

where M is the mass of the star. Using typical parameters $B = 10^{12}$G, $R = 10^6$cm, $I_{\rm p}/I_{\rm n} = 0.05$, $\Omega_0 = 2\pi/0.1\ {\rm s}^{-1}$ and $M = 1.4M_\odot$ and setting $\theta = \pi/2$ we find $\tau \approx 7\times10^4$ years.

Let us now consider the evolution of the, unseen, neutron component. From equation (35) we have

$$\Omega_{\rm n} - \Omega_{\rm n}^0 = -\frac{\varepsilon\tilde{I}}{1-\varepsilon\tilde{I}}\left(\Omega_{\rm p} - \Omega_0\right)\,, \tag{43}$$

where $\Omega_{\rm n}^0 = \Omega_{\rm n}(t=0)$. Substituting equation (39) into this we get

$$\Omega_{\rm n} \approx \Omega_{\rm n}^0 + \frac{\varepsilon\tilde{I}}{1-\varepsilon\tilde{I}}\frac{\Omega_0 t}{\tau}\,. \tag{44}$$

This relation allows us to estimate how long it takes for a rotational lag to develop between the two constituents. Assuming that the two components rotate together at time $t = 0$ then $\Omega_{\rm n}^0 = \Omega_0$. The rotational lag then evolves according to

$$\begin{aligned}\Delta\Omega = \Omega_{\rm n} - \Omega_{\rm p} &= \frac{\varepsilon\tilde{I}}{1-\varepsilon\tilde{I}}\frac{\Omega_0 t}{\tau} + \frac{\Omega_0 t}{\tau} \\ &= \left(1 + \frac{\varepsilon\tilde{I}}{1-\varepsilon\tilde{I}}\right)\frac{\Omega_0 t}{\tau} = \frac{1}{1-\varepsilon\tilde{I}}\frac{\Omega_0 t}{\tau}\,, \end{aligned} \tag{45}$$

or

$$\frac{\Delta\Omega}{\Omega_{\rm p}} \approx \frac{1}{1-\varepsilon\tilde{I}}\frac{t}{\tau}\,. \tag{46}$$

It has been argued (Lyne et al. 2000) that a rotational lag of $\Delta\Omega/\Omega_{\rm p} \approx 10^{-4}$ is needed in order to "explain" Vela sized glitches. From (46) we see

$$\frac{t}{\tau} \approx 10^{-4} \rightarrow t \sim 7 \text{ years}\,. \tag{47}$$

Hence, this simple model is consistent with large glitches occuring once in a few years in a typical young pulsar.

Finally, let us consider the entrainment coupling in more detail. In general, the evolution of the rotation of the proton and neutron fluids is given by (39) and (44), respectively. If we focus on a sufficiently short evolutionary timescale, then we can assume that $\dot{J}_{\rm em}$ is approximately constant. From equations (33)-(35) we find

$$\dot{\Omega}_{\rm p} = -\frac{1}{I_{\rm p}}\left(1 - \frac{\varepsilon I_{\rm n}}{I_{\rm n} - \varepsilon I_{\rm p}}\right)^{-1}\dot{J}_{\rm em}\,. \tag{48}$$

This is an interesting, and perhaps surprising result. It appears that, even though a spin down torque acts on the protons their rotational velocity may increase. This happens when

$$\frac{I_{\rm n}}{I_{\rm n}+I_{\rm p}} < \varepsilon < \frac{I_{\rm n}}{I_{\rm p}}\,. \tag{49}$$

Would this happen for realistic parameter values? Setting $\varepsilon = 0.05$ and $I_{\rm p}/I_{\rm n} = 0.1$, typical values in the outer neutron star core (Chamel 2006), we find that the crust should spin down. However, if we consider the neutron fluid we find the condition for spin up is

$$0 < \varepsilon < \frac{I_{\rm n}}{I_{\rm n}+I_{\rm p}}\,. \tag{50}$$

For the expected values of ε and $I_{\rm p}/I_{\rm n}$ we see that the neutron fluid spins up. This is somewhat counter-intuitive, but does not violate any fundamental principles. In fact, it is easy to see how this effect can result from an exchange of angular momentum in a coupled system. Unfortunately, since we do not observe the neutron component directly, the result does not help us constrain the entrainment parameter. It is just an example of the drastic effect that entrainment can have on the evolution of a system.

4 MODELLING A GLITCH

The two-component model that we have described cannot be used to model glitch events unless we add more physics to it. Key to the problem is the motion of the superfluid vortices. There are two aspects to this problem; We need to account for the friction that arises due to the presence of the vortices and the associated dissipative coupling between the two fluids in the model (Alpar et al. 1984; Mendell 1991; Andersson et al. 2006). We should also consider the interaction between the vortices and the nuclei in the neutron star crust, the potential pinning of the vortices to the lattice (Donati & Pizzochero 2006; Avogadro et al. 2008) and the extent to which the vortices exhibit creep in the presence of a rotational lag (Anderson & Itoh 1975; Alpar et al. 1984, 1989; Link et al. 1993; Alpar et al. 1993).

In the following, we will focus on the role of the mutual friction and the glitch event itself. The vortex pinning will be dealt with in a very simplistic fashion. We will simply assume that the vortices are either perfectly pinned or completely unpinned. In such a model, a glitch would proceed as follows. Assume that the superfluid vortices form a uniform, straight, array aligned with the rotation axis (that is, we are not considering potential vortex tangles and turbulence (Andersson et al. 2007), which would make the problem quite a lot harder since the model would have to contain local information (Peralta et al. 2005)). In this case vortex pinning simply fixes the number of vortices per unit area. This in turn fixes the neutron fluids angular momentum, so the superfluid component rotates at a constant rate. If we assume that the charged fluid is locked to the crust via magnetic effects then the vortices will be rotating with the charged fluid component. As the crust spins down due to the electromagnetic torque, a velocity difference will build up between the two constituents. This will lead to an increasing Magnus force acting on the vortices. Eventually, when some critical lag, $\Delta\Omega_{\rm c}$, is reached this force will be strong enough to overcome the nuclear pinning and the vortices are suddenly free to move. At this point the vortex mutual friction becomes relevant and serves to transfer angular momentum between the two components. This becomes the mechanism by which the

two components couple and the lag decays. The crust spins up leading to the observed glitch jump. If the system relaxes completely, the end state should be such that the two components rotate at the same rate. The glitch event itself is relatively sudden. The best resolved event to date is the so-called Christmas glitch in the Vela pulsar, where the glitch rise time was shorter than a few tens of seconds (Dodson et al. 2002). In other words, the angular momentum is transfered to the crust in less than a few hundred rotation periods. On a longer timescale one would expect the vortices to repin. After all, in the relaxed state the Magnus force is absent (or at least very small). The repinning should determine the long-term relaxation of the glitch, i.e. the spin evolution on timescales longer than tens of seconds. In order to model this phase one would likely need to account for vortex creep. Eventually, the system will reach a state where the rotational lag increases, and the pulsar may glitch again.

We focus on the glitch event itself, i.e. the short term evolution following global vortex unpinning. During this phase one would expect the main dynamics to be determined by the mutual friction force. Hence, we do not have to consider either the electromagnetic torque or the vortex creep. These are, of course, important in a complete glitch model, c.f. Larson & Link (2002) for an interesting discussion of the relaxation phase, but since they require dynamics on rather different timescales it is natural to (at least initially) consider the different phases separately. Our main aim is to compare a simple "global" glitch model to a numerical evolution that takes into account the actual hydrodynamics.

4.1 The evolution equations

To model a glitch event we need to account for the mutual friction force. As discussed by Andersson et al. (2006) this means that we consider the evolution equations

$$\mathcal{E}_i^{\rm x} = \left(\frac{\partial}{\partial t} + v_{\rm x}^j\nabla_j\right)\left(v_i^{\rm x} + \varepsilon_{\rm x} w_i^{\rm yx}\right) + \nabla_i\left(\phi + \tilde{\mu}_{\rm x}\right) + \varepsilon_{\rm x} w_j^{\rm yx}\nabla_i v_{\rm x}^j = \frac{\rho_{\rm n}}{\rho_{\rm x}}\mathcal{B}\left|\omega_{\rm n}\right| w_i^{\rm yx} - \frac{\rho_{\rm n}}{\rho_{\rm x}}\mathcal{B}'\epsilon_{ijk}\omega_{\rm n}^j w_{\rm yx}^k\,, \tag{51}$$

where $\mathcal{B}$ and $\mathcal{B}'$ are the mutual friction parameters (Andersson et al. 2006). We have assumed that the vortex array remains straight and that the rotational lag remains orthogonal to the rotation axis. This is the simplest assumption. If we were to relax it, we would have to consider possible precession of the system and the mutual friction force would be more complicated. In the case that we are considering, we have

$$\omega_i^{\rm n} = 2\Omega_i^{\rm n} + \varepsilon_{\rm n}\left(2\Omega_i^{\rm p} - 2\Omega_i^{\rm n}\right)\,. \tag{52}$$

Generalising the prescription from the previous section, we can find the energy equation for each constituent. This leads to

$$\frac{\partial E_{\rm x}}{\partial t} = \int \rho_{\rm x} v_{\rm x}^j \mathcal{E}_j^{\rm x} dV = \int \rho_{\rm x} v_{\rm x}^j\left[\mathcal{B}\frac{\rho_{\rm n}}{\rho_{\rm x}}\left|\omega_{\rm n}\right| w_j^{\rm yx} - \mathcal{B}'\frac{\rho_{\rm n}}{\rho_{\rm x}}\epsilon_{jkl}\omega_{\rm n}^k w_{\rm yx}^l\right] dV\,. \tag{53}$$

The second term in the integral will vanish as $v_i^{\rm x}$ is parallel to $w_i^{\rm yx}$. Written in terms of the moments of inertia $I_{{\rm x}i}{}^j$, cf. (26), the total change in energy is given by

$$\frac{\partial E}{\partial t} = \frac{\partial}{\partial t}\left\{\frac{1}{2}I_{\rm n}\Omega_{\rm n}\left[\Omega_{\rm n} + \varepsilon_{\rm n}\left(\Omega_{\rm p} - \Omega_{\rm n}\right)\right] + \frac{1}{2}I_{\rm p}\Omega_{\rm p}\left[\Omega_{\rm p} + \varepsilon_{\rm p}\left(\Omega_{\rm n} - \Omega_{\rm p}\right)\right]\right\} = -\mathcal{B}\left|\omega_{\rm n}\right|\left(\Omega_{\rm p} - \Omega_{\rm n}\right)^2 I_{\rm n} < 0\,. \tag{54}$$

That is, the mutual friction leads to a loss of kinetic energy (as expected). The equilibrium (minimum energy) state is reached when the two fluids are rotating together ($\Omega_{\rm p} = \Omega_{\rm n}$).

We can also calculate the global change in angular momentum. Focusing on the z-component of the angular momentum we find

$$\frac{\partial J_i^{\rm x}}{\partial t} = \int \rho_{\rm x}\epsilon_{ijk}x^j\mathcal{E}^k dV = \int \epsilon_{ijk}x^j\left[\mathcal{B}\rho_{\rm n}\left|\omega_{\rm n}\right| w_{\rm yx}^k - \mathcal{B}'\rho_{\rm n}\epsilon^{klm}\omega_l^{\rm n} w_m^{\rm yx}\right] dV\,. \tag{55}$$

Noting that

$$\epsilon_{ijk}x^j\epsilon^{klm}\omega_l^{\rm n} w_m^{\rm yx} = x_{\rm x}^j\omega_i^{\rm n} w_j^{\rm yx} - x^j\omega_j^{\rm n} w_i^{\rm yx} = 0 \quad \text{for} \quad i = z\,, \tag{56}$$

and

$$\epsilon_{ijk}x^j w_{\rm yx}^k = \epsilon_{ijk}x^j\epsilon^{klm}\Omega_l^{\rm yx}x_m = \Omega_i^{\rm yx}x^j x_j - \Omega_j^{\rm yx}x^j x_i\,, \tag{57}$$

we can write the change in angular momentum in terms of the constituent moments of inertia to get

$$\frac{\partial J_i^{\rm x}}{\partial t} = \mathcal{B}\left|\omega_{\rm n}\right|\left(\Omega_j^{\rm y} - \Omega_j^{\rm x}\right) I_{\rm n}{}_i^j\,. \tag{58}$$

The total angular momentum is given by

$$\frac{\partial J_i}{\partial t} = \frac{\partial J_i^{\rm n}}{\partial t} + \frac{\partial J_i^{\rm p}}{\partial t} = 0\,. \tag{59}$$

Hence, the angular momentum is conserved. This is as expected since no external torques have been accounted for. It is worth noting that the $\mathcal{B}'$ coefficient does not feature in the final equations.

4.2 An explicit solution

We will now solve the global evolution equations for the system. To do this, it is useful to rewrite them in terms of the rotational lag and a quantity directly related to the total angular momentum. The conservation of angular momentum makes the latter variable trivial to deal with, while the lag is a key (more or less directly observable) quantity.

From (30), (59) and assuming that the moment of inertia of each constituent remains constant, we define $\mathcal{V}$ from the angular momentum such that

$$I_{\rm n}\dot{\Omega}_{\rm n} + I_{\rm p}\dot{\Omega}_{\rm p} = I\dot{\mathcal{V}} = 0\,. \tag{60}$$

Then it is obvious that $\mathcal{V}$ remains constant during the evolution. From (30) and (58) we next find that the rate of change of the lag $\mathcal{W} = \Omega_{\rm n} - \Omega_{\rm p}$ is given by

$$(1-\bar{\varepsilon})\dot{\mathcal{W}} = \dot{\Omega}_{\rm n} - \dot{\Omega}_{\rm p} = -2(\Omega_{\rm n} - \varepsilon_{\rm n}W)\mathcal{B}\left(1 + \frac{I_{\rm n}}{I_{\rm p}}\right)\mathcal{W}\,, \tag{61}$$

where we have defined $\bar{\varepsilon} = \varepsilon_{\rm n} + \varepsilon_{\rm p}$. From (60) we can rewrite $\mathcal{V}$ as

$$\mathcal{V} = \frac{I_{\rm n}}{I}\Omega_{\rm n} + \frac{I_{\rm p}}{I}\Omega_{\rm p} = \frac{I_{\rm n}}{I}\Omega_{\rm n} + \frac{I_{\rm p}}{I}\left(\Omega_{\rm n} - \mathcal{W}\right) = \Omega_{\rm n} - \frac{I_{\rm p}}{I}\mathcal{W}\,. \tag{62}$$

Substituting this into (61) gives

$$(1-\bar{\varepsilon})\dot{\mathcal{W}} = -2\mathcal{B}\left[\mathcal{V} + \left(\frac{I_{\rm p}}{I} - \varepsilon_{\rm n}\right)\mathcal{W}\right]\frac{I}{I_{\rm p}}\mathcal{W}\,. \tag{63}$$

This is the stage at which the change of variables helps us. Because $\mathcal{V}$ is constant, equation (63) is separable. Straightforward integration, assuming that the glitch occurs at time $t = 0$ and defining $\mathcal{W}_0 = \mathcal{W}(0)$, leads to

$$\mathcal{W} = \mathcal{V}\left[\frac{\mathcal{V}}{\mathcal{W}_0}e^{t/\tau} + \left(\frac{I_{\rm p}}{I} - \varepsilon_{\rm n}\right)\left(e^{t/\tau} - 1\right)\right]^{-1}\,. \tag{64}$$

The spin-up time τ is given by

$$\tau = \frac{(1-\bar{\varepsilon})I_{\rm p}}{2\mathcal{B}I\mathcal{V}}\,. \tag{65}$$

For practical purposes it is better to express $\mathcal{V}$ in terms of the initial conditions. Defining the initial rotation of the protons as Ω_0 we easily find $\mathcal{V}$ at time $t = 0$. From (60) it follows that

$$\mathcal{V} = \frac{1}{I}\left(I_{\rm n}\Omega_{\rm n} + I_{\rm p}\Omega_{\rm p}\right) = \frac{I_{\rm n}}{I}\left(\mathcal{V} + \frac{I_{\rm p}}{I}\mathcal{W}_0\right) + \frac{I_{\rm p}}{I}\Omega_0\,. \tag{66}$$

This rearranges to give

$$\mathcal{V} = \frac{I_{\rm n}}{I}\mathcal{W}_0 + \Omega_0 \approx \Omega_0\,, \tag{67}$$

which should hold since $\mathcal{W}_0 \ll 1$. We then arrive at the final result

$$\mathcal{W} \approx \Omega_0\left[\frac{\Omega_0}{\mathcal{W}_0}e^{t/\tau} + \left(\frac{I_{\rm p}}{I} - \varepsilon_{\rm n}\right)\left(e^{t/\tau} - 1\right)\right]^{-1} \approx \mathcal{W}_0 e^{-t/\tau}\,, \tag{68}$$

where

$$\tau \approx \frac{(1-\bar{\varepsilon})I_{\rm p}}{2\mathcal{B}I\Omega_0}\,. \tag{69}$$

It is easy to show that the observed component (the protons) evolves according to

$$\Omega_{\rm p} \approx \Omega_0 + \frac{I_{\rm n}}{I}\mathcal{W}_0\left(1 - e^{-t/\tau}\right)\,. \tag{70}$$

4.3 Matching Observational Data

The model we have described is obviously quite simplistic. Most importantly, the assumption of constant parameters (which allowed us to carry out the integration over the body of the star in the first place) is quite unrealistic. Having said that, it would not be surprising if the final model were to retain some of the bulk dynamics of the more complex system. Of course, the various quantities in, for example, (69) must be take to represent "body averages" in some sense. Moreover, the model is only relevant on the relatively short timescale of the glitch jump itself. In order to describe the subsequent long-term evolution we would need to include both the the magnetic spin-down torque and the repinning of the vortex lines to the crust. The latter could possibly be accounted for by "switching off" the mutual friction "gradually". That is, one could simply take $\mathcal{B}$ to be time-dependent, reflecting the amount of vortex pinning or the nature of the vortex creep. This idea has been considered by Sidery (2008), and we think it would be interesting to develop it further.

Despite these caveats, it is interesting to consider how observations may constrain the various parameters. Let us consider the scenario where the observed component represents a small fraction of the total moment of inertia. This would be the case

for a typical neutron star crust coupled to a large superfluid reservoir in the core, when we may have $I_{\rm p}/I \sim 10^{-2}$. Then the observed glitch jump would be

$$\frac{\Omega_{\rm p} - \Omega_0}{\Omega_0} \approx \frac{I_{\rm n}}{I}\frac{\mathcal{W}_0}{\Omega_0} \approx \frac{\mathcal{W}_0}{\Omega_0}\,. \tag{71}$$

That is, $\mathcal{W}_0$ would correspond (more or less directly) to the observed glitch size. At the same time, the available constraint on the glitch rise time can be compared to the spin-up time of the model. Let us, for simplicity, impose the constraint that the glitch happens in less than 100 rotations. Then we need

$$\tau\Omega_0 \approx \frac{(1-\bar{\varepsilon})I_{\rm p}}{2\mathcal{B}I} < 10^2\,. \tag{72}$$

We can rewrite the entrainment factor in terms of the effective proton mass in the usual way (Prix et al. 2002). Then

$$\varepsilon_{\rm p} = 1 - \frac{m_{\rm p}^*}{m_{\rm p}} \qquad \longrightarrow \qquad 1-\bar{\varepsilon} \approx \frac{m_{\rm p}^*}{m_{\rm p}}\,, \tag{73}$$

and we need

$$\tau\Omega_0 \approx \frac{m_{\rm p}^*}{m_{\rm p}}\frac{I_{\rm p}}{2\mathcal{B}I} < 10^2\,, \tag{74}$$

or, for the suggested moment of inertia ratio,

$$\mathcal{B} > 5\times 10^{-5}\frac{m_{\rm p}^*}{m_{\rm p}}\,. \tag{75}$$

This constraint is not very severe. In particular, the canonical value $\mathcal{B} \sim 10^{-4}$ (Alpar et al. 1984; Mendell 1991; Andersson et al. 2006) lies within the required range. However, if we use the contraint of a spin-up of the order of a day suggested by a partially resolved glitch in the CRAB pulsar (Lyne et al. 1992), then the mutual friction parameter would be constrained to being weaker than $\mathcal{B} \sim 10^{-10}$. This result would not accord well with our current mutual friction models, likely illustrating our level of ignorance about the relevant physics.

In principle, we would now want to consider the case when the superfluid component represents only the free neutrons in the crust. That is, when we have $I_{\rm n}/I \approx 10^{-2}$ (Link et al. 1999). However, the model that we have developed does not immediately apply to this situation. This is obvious since we have assumed that two-fluid hydrodynamics applies throughout the system. In order to adress the crust superfluid problem we would have to add a component representing the single fluid core, and ensure that it is coupled to the two-fluid region in a suitable way. In particular, this core component would affect (59). This generalisation is complicated by the fact that we would have to add appropriate boundary conditions at the interfaces. As our main aim is to compare the averaged model to the detailed hydrodynamics we will leave consideration of models with distinct superfluid regions for future work.

4.4 Energetics

In the next section we will consider the hydrodynamics associated with a (core) glitch event. A key motivation for this discussion is the need to understand the actual details of how a macroscopic glitch is triggered (presumably through a large-scale instability) and how the system evolves once vortices become unpinned. By modelling the required hydrodynamics we hope to understand the nature of glitches better. We should, for example, be able to establish to what extent the simple "bulk model" we have discussed represents the behaviour of a true two-fluid system. We can also address other interesting questions, concerning for example the modes of oscillation that are excited in a glitch. This is an interesting question to ask because, first of all, there may be additional variability in the glitch event and, secondly, the fluid oscillations may be associated with gravitational-wave emission. It is obviously relevant to try to understand the nature of this gravitational-wave signal and estimate its amplitude. One should probably not expect glitching pulsar to be supreme gravitational-wave sources, but these estimates are nevertheless interesting. Most importantly, since glitches are common in young pulsars (and magnetars) it may be "reasonable" to assume that the corresponding level of energy is associated with regular dramatic events in a neutron star's life.

Let us therefore consider the energetics of the problem. In past studies, it has been common to estimate the energy available for radiation based on a single component model. In that case the total kinetic energy and angular momentum are (obviously) given by

$$E = \frac{1}{2}I\Omega^2\,, \qquad \text{and} \qquad J = I\Omega\,. \tag{76}$$

Assume that a glitch of size $\Delta\Omega$ results from a change in the moment of inertia ΔI. This would represent a "starquake" in an elastic star. Then, assuming that the total angular momentum is conserved, it is easy to show that the available energy is

$$\Delta E_1 \approx \frac{1}{2}I\Omega\Delta\Omega\,. \tag{77}$$

As discussed by, for example, Andersson & Comer (2001) this estimate suggests that pulsar glitches may be of interest for

future generations of gravitational-wave astronomers. However, if we consider the two-component model we get a rather different picture. In this case, for constant $I_{\rm x}$, the conservation of angular momentum in the glitch leads to

$$\Delta\Omega_{\rm n} = -\frac{I_{\rm p}}{I_{\rm n}}\Delta\Omega_{\rm p}\,. \tag{78}$$

That is, the superfluid (neutrons) spin down as the crust (protons) spin up. Estimating the available energy, we find that

$$\Delta E_2 \approx \frac{1}{2} I_{\rm p}(\Delta\Omega)^2\,. \tag{79}$$

Here, $\Delta\Omega = \Delta\Omega_{\rm p}$ and we have assumed that $I_{\rm p} \ll I_{\rm n}$. For typical parameters, $I_{\rm p}/I \approx 0.1$ and $\Delta\Omega/\Omega \approx 10^{-6}$, we see that

$$\Delta E_2 \sim 5 \times 10^{-8} \Delta E_1\,. \tag{80}$$

In other words, in the two-component model the energy available for radiation is much smaller than in the starquake case. Even though it is not clear how the estimate will change if we account for the energy radiated as heat, changes in internal and potential energy etcetera, it is clear that the result is rather pessimistic. If the estimate is taken seriously, and glitches really represent a transfer of angular momentum as in the two-fluid model, then the gravitational-wave signal from a pulsar glitch is unlikely to be detected by any future generation of detectors. Of course, our level of understanding of this problem is still rudimentary. We need to improve our models considerably if we are to make more reliable estimates. The simulations that we will now discuss provide an important step in this direction.

5 HYDRODYNAMICS MODEL

The "bulk" model that we have discussed so far is able to describe some key properties of glitches. However, the model has obvious restrictions. In particular, it does not provide any information whatsoever about the actual hydrodynamics of the event. By focusing on solid body motion we are obviously considering only the averaged dynamics. In principle, one would expect the result to be relevant when the dynamics is much slower than, say, the speed of sound in the fluid. However, it is clear that we need to move beyond the averaged model if we want to understand issues like the trigger mechanism for glitches, consider potential gravitational-wave signals etcetera. It is thus natural to consider the hydrodynamical aspects of the glitch problem. To do this, we have extended the numerical code that was recently developed by Passamonti, Haskell & Andersson (2009) [see Peralta et al. (2005, 2006); Peralta & Melatos (2009) for a parallel effort]. Within the two-fluid framework, we evolve perturbations of rotating, superfluid Newtonian stars in time. The new version of the code includes the effects of mutual friction and the perturbed gravitational potential (i.e. we are not working in the Cowling approximation). We initiate the time evolution with suitable conditions that mimic a pre-glitch configuration, where the two fluids rotate uniformly with different velocities. Assuming that the vortex pinning that is required to reach this state is instantaneously broken, we can evolve the system. This allows us to determine the mutual friction damping, extract the associated gravitational signal and infer the oscillation modes that are excited during a "glitch". In particular, we can test the analytical formula for the global spin-up timescale τ, equation (69).

The main motivation for our perturbative treatment is to consider stellar models where the relative velocity lag between neutrons and protons is very small as a deviation from stationary equilibrium configurations. These background models, which are such that the two fluids co-rotate, are in β-equilibrium and coexist throughout the star's volume, can be constructed by extending the standard self-consistent field method of Hachisu (1986). The details of this method, and its application to superfluid stars can be found in Yoshida & Eriguchi (2004) and Passamonti et al. (2009). In our current models the crust is neglected (for simplicity). Our aim is to continue to add key physics to the model, and we plan to consider crustal effects in future work.

Non-corotating configurations can be determined using the perturbative approach developed by Yoshida & Eriguchi (2004), where the deviations from co-rotation are numerically computed by means of a variation of the self-consistent field method. We extend this numerical approach to study different superfluid equations of state and generate rotating stellar sequences with constant mass. These non-corotating deviations are then implemented in the hydrodynamical code as initial conditions and evolved in time with a system of perturbation equations. This system is formed by the linearised versions of the two-fluid mass conservation equations, the two Euler-type equations (51) and the Poisson equation for the gravitational potential. Technical details on the construction of the initial data and the time domain numerical code will be provided elsewhere (Passamonti & Andersson 2009). Here, we report only results that can be directly compared with the analytic expressions from the previous sections.

In a two-fluid model, the relative motion between protons and neutrons can be approximately decomposed in co- and counter-moving components. With an appropriate choice of perturbation variables, we can study the effects of these two degrees of freedom on the oscillation spectrum and the factors that generate their coupling (Andersson et al. 2009; Passamonti et al. 2009).

The perturbation equations must be completed with an equation of state (EoS), which can be described by the energy

Table 1. This table provides the main parameters of the corotating background models for both the A and C sequences. The first column labels each model, while the second and third columns give, respectively, the ratio of polar to equatorial axes and the angular velocity of the star. In the fourth column, the rotation rate is compared to the Kepler velocity Ω_K that represents the mass shedding limit. The ratio between the rotational kinetic energy and gravitational potential energy $T/|W|$ is given in the fifth column. In the sixth and seventh columns we show the moment of inertia of the proton and neutron fluids, respectively, while in the eighth column we provide the stellar mass. All quantities are given in dimensionless units, where G is the gravitational constant, ρ_0 represents the central mass density and R_{eq} is the equatorial radius.

Model	R_p/R_{eq}	$\Omega/\sqrt{G\rho_0}$	Ω/Ω_K	$T/\|W\| \times 10^2$	$I_{\rm p}/(\rho_0 R_{eq}^5)$	$I_{\rm n}/(\rho_0 R_{eq}^5)$	$M/(\rho_0 R_{eq}^3)$
A0	1.00000	0.00000	0.00000	0.00000	0.03328	0.29951	1.2732
A1	0.99792	0.05913	0.08156	0.05802	0.03319	0.29868	1.2701
A2	0.98333	0.16675	0.22999	0.38482	0.03253	0.29278	1.2479
A3	0.95000	0.28799	0.39627	1.16918	0.03102	0.27915	1.1967
A4	0.93333	0.33081	0.45629	1.56885	0.03025	0.27224	1.1709
A5	0.90000	0.40268	0.55543	2.38295	0.02869	0.25822	1.1186
C0	1.00000	0.00000	0.00000	0.00000	0.01906	0.24657	1.0826
C1	0.99792	0.05586	0.08403	0.04561	0.01900	0.24584	1.0798
C2	0.98333	0.15764	0.23716	0.36682	0.01858	0.24064	1.0601
C3	0.95000	0.27145	0.40837	1.11303	0.01760	0.22861	1.0146
C4	0.93333	0.31246	0.47006	1.49236	0.01711	0.22251	0.9915
C5	0.90000	0.38006	0.57177	2.26285	0.01610	0.21009	0.9447

functional (16):

$$E = E\left(\rho_{\rm n}, \rho_{\rm p}, w_{\rm np}^2\right) , \tag{81}$$

where we have replaced the number densities $n_{\rm x}$ with the mass densities $\rho_{\rm x}$ (assuming for simplicity that the neutron and proton masses are equal, $m_{\rm p} = m_{\rm n}$). When the relative velocity between the two fluids is small, equation (81) can be expanded in a Taylor series (Prix et al. 2002; Passamonti et al. 2009). Then we have

$$E = E_0\left(\rho_{\rm n}, \rho_{\rm p}\right) + \alpha_0\left(\rho_{\rm n}, \rho_{\rm p}\right) w_{\rm np}^2 + \mathcal{O}\left(w_{\rm np}^4\right) , \tag{82}$$

where the entrainment function, α_0, and the bulk equation of state, E_0, can be independently specified on the corotating background, where $w_{\rm pn}^i = 0$. In this paper, we consider two sets of polytropic superfluid equations of state already used by Passamonti et al. (2009). Despite their simplicity, these models are very useful for investigating the effects of the different physical parameters on the oscillation dynamics. In particular, one of these two classes of equation of state describes models with composition gradients that couple the co- and counter-moving degrees of freedom.

The first equation of state is given by the following expression:

$$E_0 = \frac{K}{1-(1+\sigma)\,x_{\rm p}}\rho_{\rm n}^2 - \frac{2K\sigma}{1-(1+\sigma)\,x_{\rm p}}\rho_{\rm n}\rho_{\rm p} + \frac{K\left[1+\sigma-(1+2\sigma)\,x_{\rm p}\right]}{x_{\rm p}\left[1-(1+\sigma)\,x_{\rm p}\right]}\rho_{\rm p}^2 , \tag{83}$$

where K and the proton fraction $x_{\rm p}$ are taken to be constant. As discussed by Prix et al. (2002), the parameter σ is related to the "symmetry energy" of the EoS. For this model, we have constructed a sequence of co-rotating axisymmetric configurations which do not have composition gradients. These non-stratified stars correspond to the A models used by Passamonti et al. (2009). Table 1 gives the main quantities of some rotating models that we consider in this paper. Details for more rapidly rotating models can be found in Passamonti et al. (2009).

The second analytical equation of state, that describes stratified superfluid stars, can be written (Prix & Rieutord 2002; Andersson et al. 2002; Passamonti et al. 2009):

$$E_0 = k_{\rm n}\,\rho_{\rm n}^{\gamma_n} + k_{\rm p}\,\rho_{\rm p}^{\gamma_{\rm p}} . \tag{84}$$

In this paper we determine a sequence of rotating stars, whose non-rotating member is Model III of Prix & Rieutord (2002). For our polytropic models we use $\gamma_{\rm n} = 1.9$ and $\gamma_{\rm p} = 1.7$, while the coefficients $k_{\rm x}$ are given, in units $GR_{eq}\rho_0^{2-\gamma_x}$, by $k_{\rm n} = 0.682$ and $k_{\rm p} = 3.419$, respectively. Recall that G, R_{eq} and ρ_0 are the gravitational constant, the equatorial radius and the central mass density, respectively. Imposing β-equilibrium on the corotating background model, we can determine the proton fraction as (Prix & Rieutord 2002; Passamonti et al. 2009):

$$x_{\rm p} = \left[1 + \frac{\left(\gamma_{\rm p}k_{\rm p}\right)^{N_{\rm p}}}{\left(\gamma_{\rm n}k_{\rm n}\right)^{N_{\rm n}}}\,\tilde{\mu}^{N_{\rm n}-N_{\rm p}}\right]^{-1} , \tag{85}$$

where $N_{\rm n}$ and $N_{\rm p}$ are the neutron and proton polytropic indices of the EoS, defined as $N_{\rm x} = (\gamma_{\rm x}-1)^{-1}$. For this model, a sequence of rotating stars can then be determined via the self-consistent field method (Passamonti et al. 2009; Passamonti & Andersson 2009). We refer to these stars as models C, in order to distinguish them from the models B used by Passamonti et al. (2009). See Table 1 for some of the rotating configurations for this model.

5.1 Glitch initial data

According to the two-fluid model, a glitch brings a star with an initial velocity lag between protons and neutrons to a co-rotating configuration. The observed glitch jump is very small, $\Delta\Omega/\Omega \ll 1$, and can be associated with angular momentum transfer from the superfluid neutrons to the proton component. Regardless of the physical mechanism that generates the original velocity difference, we can describe the initial conditions for a glitch as an axisymmetric configuration where protons and neutrons rotate with a small relative velocity. If we assume that this relative rotation is aligned with the "background" rotation axis, we can use the perturbative approach developed by Yoshida & Eriguchi (2004) to determine the difference between the initial non-corotating configuration and the final corotating background.

As we have already discussed, the observed variation of the star's angular velocity during a glitch can be associated with the proton velocity. In fact, due to the magnetic field coupling between the crust and core protons, we can assume that all charged particles corotate. Meanwhile, the velocity of the superfluid neutrons must be determined from the conservation laws. If we assume that the angular momentum of the two-fluid system is conserved during a glitch, then the initial relative amplitude between the proton and neutron perturbations can be determined from

$$\sum_{\rm x} \Delta J_{\rm x} = 0\,, \tag{86}$$

where the perturbed angular momentum of the x component is given by

$$\Delta J_{\rm x} = I_{\rm x}\Delta\Omega_{\rm x} + \Delta I_{\rm x}\,\Omega\,, \tag{87}$$

and $I_{\rm x}$ is the moment of inertia of the x fluid in the corotating configuration, which rotates with angular velocity Ω. We determine the perturbation $\Delta I_{\rm x}$ from

$$\Delta I_{\rm x} = \int_0^{\mathbf{r}} \delta\rho_{\rm x}\,(r'\sin\theta)^2 d\mathbf{r}'\,, \tag{88}$$

where $\delta\rho_{\rm x}$ is the Eulerian perturbation of the mass density. From equation (86) we then have

$$I_{\rm n}\Delta\Omega_{\rm n} + I_{\rm p}\Delta\Omega_{\rm p} + (\Delta I_{\rm n} + \Delta I_{\rm p})\,\Omega = 0\,, \tag{89}$$

which leads to the following expression for the initial fluid angular velocities:

$$\frac{\Delta\Omega_{\rm p}}{\Omega} = \left.\frac{\Delta\Omega}{\Omega}\right|_{obs}\,, \tag{90}$$

$$\Delta\Omega_{\rm n} = -\frac{1}{I_{\rm n}}\left(I_{\rm p}\Delta\Omega_{\rm p} + \Delta I\,\Omega\right)\,, \tag{91}$$

where $\Delta I = \Delta I_{\rm p} + \Delta I_{\rm n}$.

For any corotating background we can determine the non-corotating corrections to the mass density $\delta\rho_{\rm x}$, the chemical potential $\delta\tilde{\mu}_{\rm x}$ and the gravitational potential $\delta\phi$ via the Yoshida & Eriguchi (2004) approach, see Passamonti & Andersson (2009) for more details. In a spherical coordinate basis, the initial velocity fields are then given by

$$\delta v^i_{\rm x} = -\Delta\Omega_{\rm x}\,\varphi^i\,. \tag{92}$$

This initial data is close to that considered in the bulk dynamics model of the previous section. Hence, we can meaningfully compare the results of our time evolutions to the averaged results. This comparison will give us a better idea of the validity of the solid-body approach. Of course, by solving the hydrodynamics problem we will be able to proceed beyond the averaged model and discuss other interesting issues.

5.2 Spin-up time

Let us first compare the mutual friction damping extracted from the time-evolution to the body averaged analytical formula (69). Considering the sequence of non-stratified models A, we test the dependence of τ on the mutual friction strength $\mathcal{B}$, the background angular velocity Ω, the moment of inertia ratio $I_{\rm p}/I$ and the entrainment parameter $\bar{\varepsilon}$. For the corotating background A models given in Table 1, we determine the initial condition for the time evolution code that corresponds to a "typical" glitch jump $\Delta\Omega/\Omega = 10^{-6}$. The related neutron velocity lag is then given by equation (91). It is worth noting that the method used to construct the initial data is linear in the two fluid velocities. This means that the results can be rescaled to other values of the glitch size.

If we exclude the mutual friction term, the numerical evolutions preserve the initial lag between protons and neutrons. At the same time, the initial conditions excite low level oscillations. This is expected as we are mapping a non-corotating axisymmetric configuration onto an axisymmetric corotating background. When mutual friction is switched on, the counter-moving motion is damped, leading to a corotating configuration on a timescale of order τ. We determine the spin-up timescale by monitoring the φ component of the velocity difference $w^i_{\rm pn}$, assuming that it depends on time as $w^\varphi_{\rm pn} = w^\varphi_{\rm pn}\,(t=0)\;e^{-t/\tau}$. By taking the natural logarithm, we can extract τ from a linear fit of the time evolved data.

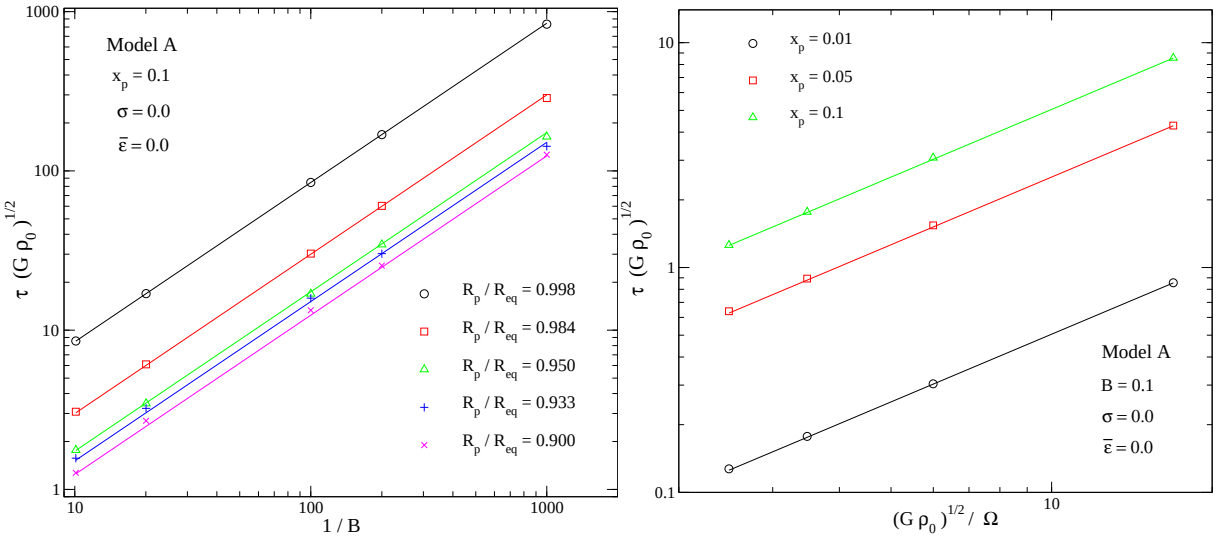

Figure 1. This figure shows the spin-up time τ as a function of the inverse of the mutual friction parameter $\mathcal{B}$ (left panel) and the background rotation rate of the star Ω (right panel) for the sequence of rotating models A. The solid lines show the behaviour predicted by equation (69), while the symbols (see legend) represent the values of the spin-up time extracted from the hydrodynamical simulations. The physical quantities are given in dimensionless units by using the gravitational constant G and the central mass density ρ_0. The axes use logarithmic scales. All the five models A1-A5 shown in this figure have both vanishing symmetry energy term σ and entrainment parameter $\bar{\varepsilon}$. In the left panel, the proton fraction is fixed to $x_{\rm p} = 0.1$ and the mutual friction is varied. Meanwhile, in the right panel we show three sequences of rotating stars with the same mutual friction strength $\mathcal{B} = 0.1$, but with three different values of proton fraction, namely $x_{\rm p} = 0.1, 0.05$ and $x_{\rm p} = 0.01$. In all cases, the numerical values of spin-up time show a good agreement with the analytical result.

In Figs. 1 and 2, we show the agreement of the numerical results with the analytical formula (69). In the left panel of Fig. 1, we consider several rotating A models with vanishing symmetry energy and entrainment and with constant proton fraction $x_{\rm p} = I_{\rm p}/I = 0.1$. The models have different mutual friction strength, controlled by the parameter $\mathcal{B}$ that we take to be constant throughout the star. The expected linear dependence of τ on the inverse of the mutual friction parameter is confirmed by the hydrodynamical simulations. In the right panel of Fig. 1, we fix instead the mutual friction strength, $\mathcal{B} = 0.1$, a rather large value, and study three sequences of rotating models with different proton fraction, respectively $x_{\rm p} = 0.01, 0.05$ and 0.1. The mutual friction damping time exhibits the expected linear dependence on Ω^{-1}. For models A1 and A2 we test also the dependence of τ on the entrainment parameter $\bar{\varepsilon}$, see Fig 2. In this case, the other stellar parameters are, respectively, $x_{\rm p} = 0.1$, $\mathcal{B} = 0.1$ and $\sigma = 0$. The linear dependence on $1-\bar{\varepsilon}$ is clearly confirmed by the evolutions. According to equation (69), the damping time should not depend (explicitly) on the symmetry energy, σ. We have carried out simulations with different σ to confirm this result.

Next, we consider the stratified models C. The aim is to establish to what extent equation (69) still provides accurate results for the spin-up time. On the one hand, one may not expect this to be the case since the various parameters in the model are no longer uniform. On the other hand, the simple prescription could still work provided that the parameters are interpreted in a body-averaged sense. We consider initial configurations with $\Delta\Omega/\Omega = 10^{-6}$ and determine the non-corotating corrections using the method discussed in Section 5.1. For the three rotating models C1-C3, the dependence of the numerical damping time on the mutual friction parameter $\mathcal{B}$ is shown in the right panel of Fig. 2. Again, the results agree well with the analytical formula (69). However, a closer examination of the data reveals that equation (69) is more accurate for the non-stratified A models. For the first three rotating models of the two sequences A and C, we show in Fig. 3 the relative deviation between the numerical and analytical spin-up time for different mutual friction strengths. Comparing models with the same axis ratio, the error is generally smaller for models A (filled symbols).

In general we find that the agreement between the numerical and analytical spin-up time is better for slowly rotating models that have strong mutual friction. In these cases, the damping of $w^i_{\rm pn}$ is less contaminated by the excitation of axisymmetric oscillations, and the numerical extraction of τ is more accurate.

5.3 Gravitational Waves

So far we have discussed "global" dynamics, e.g. how the two components in the system relax to a co-rotating configuration due to the mutual friction. We now turn to the actual hydrodynamics, and consider to what extent this kind of glitch event radiates gravitational waves. We have already established that these events are unlikely to be strong emitters of gravitational radiation. However, it seems inevitable that they should radiate at some level and it is important to establish what that level

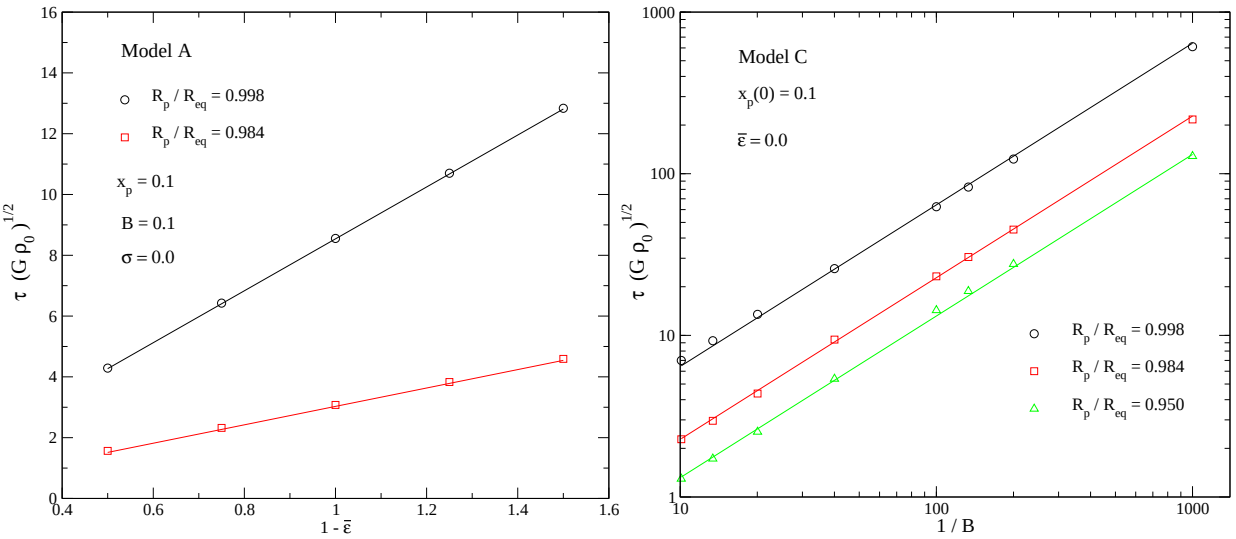

Figure 2. In this figure we compare the numerical spin-up time τ with the analytical formula (69). The values extracted from the numerical code are shown as open symbols (see legend), while the solid lines denote the analytical τ. In the left panel, we consider the two models A1 and A2, with proton fraction $x_{\rm p} = 0.1$, vanishing symmetry energy $\sigma = 0$ and constant mutual friction parameter $\mathcal{B} = 0.1$. The dependence of the numerically determined τ on the entrainment parameter agrees very well with the analytical result. In the right panel, we show (on a log-log scale) the damping time τ as a function of $\mathcal{B}^{-1}$ for the three models C1-C3 with vanishing entrainment. The agreement between the numerical and analytical spin-up times is still good, although less accurate than for the A models. See Fig. 3 and the main text for further discussion.

may be. In particular, since there are a number of glitching pulsars in the Galaxy. The energy involved in glitches indicates how energetic "typical" events in a mature neutron star may be. In that way, these events provide interesting benchmarks for gravitational-wave modelling. It is, however, important to state already from the outset that we are not expecting the mechanism that we are considering here to lead to detectable signals. This is essentially because of the high level of symmetry in the initial and final configurations, and the fact that we are assuming global vortex unpinning. The result may be quite different if we were to model localized unpinning events. Although of great interest, this problem is unfortunately beyond the reach of our current computational technology.

We will focus on the gravitational signal associated with the $l = 2$ axisymmetric oscillations that are excited in our glitch evolutions. At the linear perturbation level, the initial data excites a number of the neutron star's oscillation modes. Hence, a key question concerns which modes we expect to be present in the gravitational signal. For a single fluid star, the general mode classification is based on the main restoring force that acts on the displaced fluid elements (Cowling 1941). In this work we consider "acoustic modes" that are mainly restored by pressure variations. Since any perturbation of a spherical star can be decomposed in vector harmonics, an oscillation mode can be labeled by the harmonic indices (l, m) associated with the spherical harmonics $Y_l^m(\theta, \phi)$. This description can be extended to rotating stellar models, as the modes can be tracked back to the non-rotating limit. For any value of (l, m), the oscillation modes can be ordered by the number of radial nodes in their eigenfunctions. For acoustic modes, we then have the fundamental mode ${}^l\mathrm{f}$ with no nodes and the series of pressure modes ${}^l\mathrm{p}_i$ with i nodes.

Our glitch model leads to axisymmetric initial data. Therefore, we can only excite the family of axisymmetric modes, with $m = 0$. The quadrupole, $l = 2$, oscillations are expected to be dominant in the gravitational signal. However, in rotating stars the gravitational-wave spectrum can also contain $l = 0$ "quasi-radial" oscillation modes. In the non-rotating limit, these become purely radial modes, which do not generate gravitational radiation. The quasi-radial fundamental mode will be denoted by F and its i overtones by H_i.

In a two-fluid model the oscillation spectrum is richer, as the displaced fluid elements can now oscillate in phase and counter-phase. The comoving degrees of freedom generate oscillation modes that are similar to those of a single fluid star, and are referred to as "ordinary modes". The counter-moving degree of freedom produce a new class of modes known as "superfluid modes". In our discussion, ordinary and superfluid modes will be labeled with an upper index, for instance the $l = 2$ fundamental ordinary mode will be expressed as ${}^2\mathrm{f}^{\mathrm{o}}$, while the superfluid mode as ${}^2\mathrm{f}^{\mathrm{s}}$.

In a two-fluid star, the gravitational radiation is entirely generated by the co-moving degree of freedom (Andersson et al. 2009). We determine the gravitational strain from the standard quadrupole formula (Thorne 1980):

$$h_+^{20} = \frac{G}{c^4}\frac{1}{r}\frac{d^2\mathcal{I}}{dt^2}^{20} T_{\theta\theta}^{E2,20}\,, \tag{93}$$

where the $(l,m)=(2,0)$ pure spin tensor harmonic is given by

$$T^{E2,20}_{\theta\theta} = \frac{1}{8}\sqrt{\frac{15}{\pi}}\sin^2\theta\,. \tag{94}$$

The mass quadrupole moment for the two-fluid star is defined by (Andersson et al. 2009):

$$\mathcal{I}^{20} = 8\sqrt{\frac{\pi}{15}}\int d\mathbf{r}\,\delta\rho\, r^2 P^{20} = 8\sqrt{\frac{\pi}{15}}\int d\mathbf{r}\,\left(\delta\rho_{\rm n}+\delta\rho_{\rm p}\right) r^2 P^{20}\,, \tag{95}$$

where P^{20} is the associated Legendre polynomial:

$$P^{20} = \frac{3\cos^2\theta-1}{2}\,. \tag{96}$$

In equation (93), the numerical calculation of the second order time derivative of the quadrupole moment may lead to inaccuracies. However, the gravitational-wave extraction can be improved by using the dynamical equations and replacing the time derivative by spatial derivatives (Finn & Evans 1990). In our perturbative analysis, we have found accurate results already with the momentum-formula, where only first time derivatives appear. More details and tests will be given by Passamonti & Andersson (2009).

We rewrite equation (93) as follows:

$$h^{20}_{+} = \frac{G}{c^4}\frac{\sin^2\theta}{r}\sum_{\rm x} A^{20}_{\rm x}\,, \tag{97}$$

where the quantity $A^{20}_{\rm x}$ is given by (Passamonti & Andersson 2009)

$$A^{20}_{\rm x} \equiv 8\pi\frac{d}{dt}\int_0^{\pi/2}\sin\theta d\theta\int_0^R r^3 dr\,\rho_{\rm x}\left(\delta v^r_{\rm x}\,P^{20} + r\frac{\delta v^\theta_{\rm x}}{2}\frac{\partial P^{20}}{\partial\theta}\right)\,. \tag{98}$$

The energy radiated in gravitational waves can be determined from the following equation (Thorne 1980):

$$E_{rad} = \frac{1}{32\pi}\frac{G}{c^5}\int_{-\infty}^{\infty}\left|\frac{d^3\mathcal{I}^{20}}{dt^3}\right|^2 dt = \frac{2}{15}\frac{G}{c^5}\int_{-\infty}^{\infty}\left|\frac{dA^{20}}{dt}\right|^2 dt = \frac{16}{15}\pi^2\frac{G}{c^5}\int_0^\infty \nu^2\left|\hat{A}^{20}\right|^2 d\nu\,, \tag{99}$$

where $A^{20}=A^{20}_{\rm n}+A^{20}_{\rm p}$, and $\hat{A}^{20}$ is its Fourier transform. The energy spectrum is then given by

$$\frac{dE}{d\nu} = \frac{G}{c^5}\frac{16}{15}\pi^2\nu^2\left|\hat{A}^{20}\right|^2\,, \tag{100}$$

and the characteristic gravitational-wave strain is defined as (Flanagan & Hughes 1998):

$$h_c\left(\nu\right) \equiv \sqrt{\frac{G}{c^3}}\frac{\sqrt{2}}{\pi}\frac{1}{d}\sqrt{\frac{dE}{d\nu}} = \frac{G}{c^4}\sqrt{\frac{32}{15}}\frac{\nu}{d}\left|\hat{A}^{20}\right|\,. \tag{101}$$

In our analysis, we focus on the two rapidly rotating models A2 and C2, which rotate at a significant fraction of the mass shedding limit $\Omega/\Omega_K = 0.23$ (see Table 1 for more details). For a typical neutron star with mass $M=1.4M_\odot$ and radius $R_{eq}=10$ km, the rotation period of the A2 and C2 models is about $P\simeq 3$ ms. These models are therefore rotating much faster than all known glitching pulsars. We will demonstrate that the generation of gravitational waves is very small even for these relatively rapidly rotating models. The result can be considered as an upper limit for real glitching neutron stars. Moreover, we will show that the gravitational signal of slower rotating models can be determined by a simple rescaling of the A2 and C2 signals.

At the linear perturbation level, the entrainment parameter $\bar{\varepsilon}$ can be chosen independently from the background model. Recent work suggests that this parameter can assume values in the range $0.2\leqslant\bar{\varepsilon}\leqslant 0.8$ (Chamel 2008). The effect of the entrainment on the oscillation spectrum has been extensively studied by Prix & Rieutord (2002) and Passamonti et al. (2009). The oscillation modes that are mainly affected by $\bar{\varepsilon}$ are the so-called "superfluid" modes, which are associated with the counter-moving degree of freedom. Simple relations between the frequencies of the superfluid acoustic and inertial modes and the entrainment parameter $\bar{\varepsilon}$ have been obtained by Andersson et al. (2009); Passamonti et al. (2009); Haskell et al. (2009). In this work we show results only for the $\bar{\varepsilon}=0.5$ case, as apart from the spectral properties discussed above, we did not find any qualitative difference in simulations using other values of this parameter.

With the method discussed in Section 5.1, we set up initial data that mimic the configuration of an axisymmetric glitch. The initial value for the proton and neutron angular velocity can be determined from equations (90)-(91), once we fix the glitch size $\Delta\Omega/\Omega$ and solve the stationary equations for the background model. We will consider the case of a large glitch, where $\Delta\Omega_{\rm p}/\Omega=10^{-6}$. This means that, due to angular momentum conservation, the neutron fluid slows down with $\Delta\Omega_{\rm n}/\Omega=-1.11\times10^{-7}$ for model A2 and $\Delta\Omega_{\rm n}/\Omega=-7.74\times10^{-8}$ for model C2. Note that we use a first order perturbative framework, where for a given corotating background model the results of the time evolutions are linear with respect to the parameter $\Delta\Omega_{\rm p}/\Omega$. Hence, the gravitational-wave strain can be rescaled to any desired glitch magnitude. Furthermore, for slower rotating models that have the same glitch size, $\Delta\Omega_{\rm p}/\Omega$, we expect the perturbations and the gravitational strain to exhibit a quadratic dependence on the background rotation rate Ω. Our numerical simulations reproduce this behaviour when

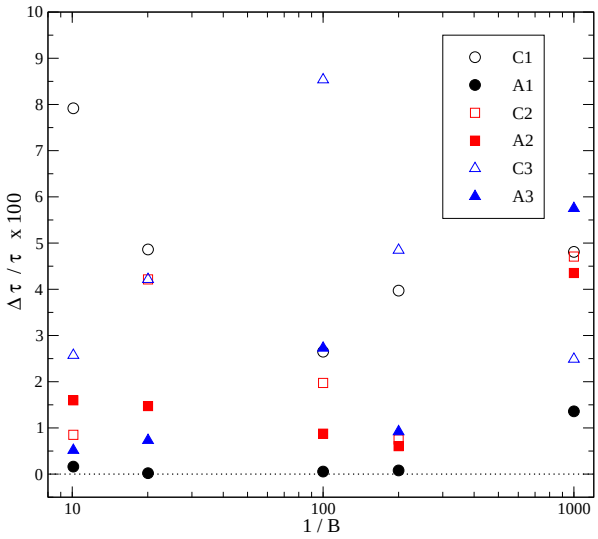

Figure 3. In this figure, we estimate the agreement between the analytical spin-up time τ from equation (69) and the values extracted from the hydrodynamical code. We show the relative deviation $\Delta\tau/\tau$ as a function of the inverse of the mutual friction parameter $\mathcal{B}$. The horizontal axis is on logarithmic scale. The results for models A and C are shown as filled and open symbols, respectively (see legend for details).

the stars have small rotational deformations, as in the case of the A1-A2 and C1-C2 models. Already for models A3 and C3, this scaling with Ω^2 is less clear and obviously it is not expected to hold for more rapidly rotating stars. In conclusion, from the evolutions of the A2 and C2 models, we can easily estimate the gravitational strain emitted by other slowly rotating models with different glitch size and background rotation.

In Fig. 4 we show the characteristic strain h_c for the A2 and C2 models with $\Delta\Omega_{\rm p}/\Omega = 10^{-6}$. The results refer to a star with mass $M = 1.4M_\odot$, radius $R_{eq} = 10$ km and with a low level of mutual friction. We consider an evolution that lasts for ~ 27.25 ms and extract the signal at 1 kpc[2]. This is roughly the distance to the Vela pulsar. The first key result in Fig. 4 is that the gravitational signal of the C2 model is about ten orders of magnitude larger than that of the A2 model. This is an enormous difference, given that these ought to be the same kind of events. The difference is due to the presence of composition gradients in the C models. In a stratified model, the co- and counter-moving degrees of freedom are coupled during the evolution. This coupling is crucial, since only the co-moving motion generates gravitational radiation. The initial data for the pre-glitch lag between neutrons and protons, in accordance with equations (90)-(91), represent a counter flow. Hence, in the non-stratified A models these conditions generate a purely counter-moving motion between the two components that does not produce any gravitational signal at all. The fact that the strain of model A2 is not completely zero in the left panel of Fig. 4 is likely due to numerical errors. In fact, we have established that the level of radiation decreases with increased resolution. The result shown for model A2 corresponds to an initial non-corotating configuration where the variation of the total rotational kinetic energy is $\Delta E_{rot}/E_{rot} \simeq 10^{-20}$. If we increase the precision of the self-consistent field method that provides the initial data we can lower this value and consequently the gravitational signal converges to zero. Moreover, the numerical noise in the simulation excites some oscillation modes that are related to the co-moving motion. In the left panel of Fig. 4 we identify the fundamental $l = 2$ mode ^{2}f, the first two pressure modes ^{2}p$_1$ and ^{2}p$_2$, and the quasi-radial fundamental mode F with its first overtone H$_1$.

Let us contrast the results for the non-stratified A2 model with the results for model C2. In this case, the chemical coupling between the two fluids introduces a co-moving motion already in the initial data. The evolutions then generate a larger gravitational strain and several oscillations modes, like the fundamental $l = 0$ and $l = 2$ modes and their respective overtones. In particular, in the right panel of Fig 4 we note that both ordinary and superfluid modes are present in the gravitational radiation. This is due to the coupling of the degrees of freedom (the oscillation modes are no longer purely co- or counter-moving). The mode frequencies of the non-rotating model C0 have been compared with the results of Prix & Rieutord (2002). The two results agree to better than 1.4% (see Passamonti & Andersson 2009). We have identified the oscillation modes

[2] It is worth noting that we have evolved the system for approximately ten rotation periods. We did not extend the evolutions because, in reality, one would expect the coupling of the two components to start playing a role at this stage. If this were not the case and the oscillation prevailed for the entire timescale of gravitational-wave damping, then the f-mode may last a few seconds. This would be about a factor of 100 longer than our evolution, meaning that the effective gravitational-wave strain could increase by perhaps an order of magnitude. It would still be too weak to be detectable.

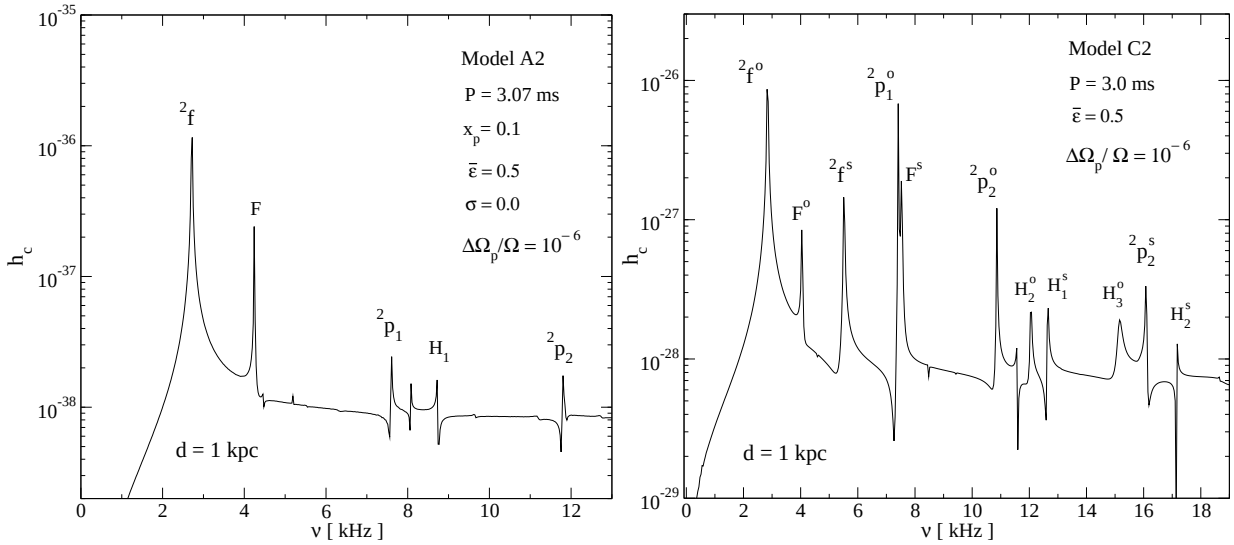

Figure 4. This figure displays the gravitational-wave signal generated by our hydrodynamical glitch simulations for the two models A2 (left panel) and C2 (right panel). On the horizontal and vertical axes we plot the oscillation frequencies and the characteristic strain extracted at a distance of 1 kpc from the source. We consider a neutron star with typical mass $M = 1.4M_\odot$ and radius $R_{eq} = 10$ km. Models A2 and C2 then correspond to stars with rotation period $P = 3.07$ ms and $P = 3.00$ ms, respectively. The other stellar parameters are $\bar{\varepsilon} = 0.5$ for the entrainment and $\sigma = 0$ for the symmetry energy. In the case of model A2 the proton fraction is constant, $x_{\rm p} = 0.1$, while model C2 is stratified with central proton fraction $\mathrm{x_p}(0) = 0.1$. The initial configuration corresponds to a large glitch with $\Delta\Omega_{\rm p}/\Omega = 10^{-6}$, as described in the main text. We run the simulation for about 27.25 ms, i.e. about 9 rotation periods, and neglect the mutual friction force. From the displayed results, the strong effects of the stratification on both the oscillation spectrum and gravitational-wave amplitude are evident.

of the C2 model by carrying out simulations with different values for the entrainment $\bar{\varepsilon}$ and tracking the superfluid modes as the parameter changes. To this end, we have also used the analytical formulae determined by Passamonti et al. (2009).

6 CONCLUDING REMARKS

We have discussed the dynamics of pulsar glitch events from two, complementary, points of view. First we constructed a simple model based on global "averaging" of the standard two-fluid equations including the mutual friction due to superfluid vortices. This analysis provides a more detailed derivation of the phenomenological relations that have been used in many discussions of glitches. In particular, our final relations clarify how the spin-up time depends on key parameters like the entrainment. The derivation also highlights the various assumptions and the restricted validity of the model. Anyway, for typical values of the parameters (see Sec. 4.3), our model has a glitch rise time shorter than the upper bound set by current observations. The model provides a useful description of the actual glitch event, but it does not account for the subsequent long-term relaxation (on a timescale of days to months) of the system. A key conclusion from our discussion is that the late stages of evolution requires additional assumptions, most likely, concerning the repinning of vortices. Understanding this phase better, e.g. connecting it to the two-fluid hydrodynamics and the averaged forces that act on the vortices, is an important challenge for the future. It seems clear that vortex creep will play a central role (Anderson & Itoh 1975; Alpar et al. 1984, 1989; Link et al. 1993; Alpar et al. 1993), but this mechanism has not yet been discussed in terms of the macroscopic hydrodynamics. This issue needs to be addressed if we are to develop more detailed models of glitch dynamics. We definitely need to move beyond phenomenology.

As a first step towards hydrodynamic glitch modelling, we have extended the recent linear perturbation evolution code of Passamonti et al. (2009) to include the mutual friction and the perturbed gravitational potential. Initiated with perturbations that represent two fluids rotating uniformly at different rates, the numerical code shows how the system relaxes to co-rotation. We have analysed this relaxation in detail and demonstrated that the behaviour is accurately described by the phenomenological model, at least for non-stratified stellar models. When the star is stratified (e.g. has varying composition) the relaxation deviates from the simple model. This is as expected, since the global model was derived under the assumption of uniform parameters. Of course, the numerical evolutions provide us with a useful tool for studying the behaviour of more complex stellar models. In addition, our time evolutions provide a first insight into the excitation of neutron star oscillations by glitches. Our results show that a set of axisymmetric modes are excited by the glitch initial data. These modes will radiate

gravitational waves[3], and it is important to establish if the associated signals may be observable with future detectors. In this respect, our results are quite pessimistic. In the cases that we have considered, the gravitational-wave signal is too weak to be detectable (even with a third generation of detectors)[4]. However, it is not clear that this is the final say on the matter. One should keep in mind that the gravitational-wave strain differs enormously for our two model configurations. The non-stratified model does not (in principle) radiate at all, while the stratified model leads to a qualitatively interesting (albeit weak) signal. The enormous difference between these results shows that we need to continue to refine our modelling. We obviously have to account for the variation of composition throughout the star, and consider the fact that superfluid components will only be present in specific density regions. We also need to understand the nature of the vortex pinning better. In our models we have assumed that the vortices unpin in a catastrophic global event. It is far from clear that this is the case in a real system. It could, for example, be that the unpinning is localized. This would make the event less symmetric which may enhance the gravitational-wave signal. We clearly need to understand the actual mechanism that triggers the glitches better. The superfluid instability discussed by Glampedakis & Andersson (2009) is interesting in this respect, but we need to study this mechanism in more detail to establish to what extent it can operate in a real neutron star.

To make progress we need to overcome a number of challenges. Yet, recent developments have provided us with interesting insights and (most importantly) computational technology that should allow us to study much more realistic neutron star models in the not too distant future.

ACKNOWLEDGEMENTS

T.S. is suported by a post-doc fellowship from EU FP6 Transfer of knowledge project 'Astrophysics of Neutron Stars' (ASTRONS, MTKD-CT-2006-042722) at Sabanci university. NA acknowledges support from STFC via grant number PP/E001025/1.

REFERENCES

Alpar M. A., Anderson P. W., Pines D., Shaham J., 1981, *ApJ*, 249, L29
Alpar M. A., Chau H. F., Cheng K. S., Pines D., 1993, *ApJ*, 409, 345
Alpar M. A., Cheng K. S., Pines D., 1989, *ApJ*, 346, 823
Alpar M. A., Langer S. A., Sauls J. A., 1984, *ApJ*, 282, 533
Alpar M. A., Pines D., Anderson P. W., Shaham J., 1984, *ApJ*, 276, 325
Anderson P. W., Itoh N., 1975, *Nature*, 256, 25
Andersson N., Comer G. L., 2001, Physical Review Letters, 87, 241101
Andersson N., Comer G. L., 2006, Classical and Quantum Gravity, 23, 5505
Andersson N., Comer G. L., Langlois D., 2002, *Phys. Rev. D*, 66, 104002
Andersson N., Comer G. L., Prix R., 2003, Physical Review Letters, 90, 091101
Andersson N., Glampedakis K., Haskell B., 2009, *Phys. Rev. D*, 79, 103009
Andersson N., Glampedakis K., Samuelsson L., 2009, *MNRAS*, 396, 894
Andersson N., Sidery T., Comer G. L., 2006, *MNRAS*, 368, 162
Andersson N., Sidery T., Comer G. L., 2007, *MNRAS*, 381, 747
Avogadro P., Barranco F., Broglia R. A., Vigezzi E., 2008, Nuclear Physics A, 811, 378
Carter B., Chamel N., 2004, International Journal of Modern Physics D, 13, 291
Carter B., Chamel N., Haensel P., 2005, Nuclear Physics A, 748, 675
Chamel N., 2006, Nuclear Physics A, 773, 263
Chamel N., 2008, *MNRAS*, 388, 737
Chamel N., Carter B., 2006, *MNRAS*, 368, 796
Cowling T. G., 1941, *MNRAS*, 101, 367
Dodson R. G., McCulloch P. M., Lewis D. R., 2002, *ApJ*, 564, L85

[3] In principle, the induced oscillations may also lead to variations in the electromagnetic signal. However, in order to quantify this effect one would need a more detailed analysis of the coupling between the motion of the crust and the magnetosphere. Such estimates are beyond the scope of the present analysis, but it is worth noting that the oscillation modes that we consider are all in the kHz range (much faster than the spin-period) meaning that they would not be seen as "modulations" of the pulsar signal.

[4] At first sight this conclusion seems at variance with the results of van Eysden & Melatos (2008), who consider a different glitch scenario. In their (cylindrical) model problem the gravitational-waves are associated with the large scale Ekman flow that results from a rotational lag between the crust and the core in the star. The two mechanisms are obviously different. In particular, in our case the event is impulsive and one would expect the signal to be burst-like. We certainly cannot envisage the 14 day integration suggested by van Eysden & Melatos (2008) to improve the signal to noise ratio. Basically, the model parameters used by van Eysden & Melatos (2008) seem rather optimistic.

Donati P., Pizzochero P. M., 2006, Physics Letters B, 640, 74
Finn L. S., Evans C. R., 1990, *ApJ*, 351, 588
Flanagan É. É., Hughes S. A., 1998, *Phys. Rev. D*, 57, 4535
Glampedakis K., Andersson N., 2009, Physical Review Letters, 102, 141101
Gusakov M. E., Haensel P., 2005, Nuclear Physics A, 761, 333
Hachisu I., 1986, *ApJS*, 62, 461
Haskell B., Andersson N., Passamonti A., 2009, *MNRAS*, 397, 1464
Larson M. B., Link B., 2002, *MNRAS*, 333, 613
Lattimer J. M., Prakash M., 2004, Science, 304, 536
Link B., 2003, Physical Review Letters, 91, 101101
Link B., Epstein R. I., 1996, *ApJ*, 457, 844
Link B., Epstein R. I., Baym G., 1993, *ApJ*, 403, 285
Link B., Epstein R. I., Lattimer J. M., 1999, Physical Review Letters, 83, 3362
Lyne A. G., Shemar S. L., Smith F. G., 2000, *MNRAS*, 315, 534
Lyne A. G., Smith F. G., Pritchard R. S., 1992, *Nature*, 359, 706
Melatos A., Peralta C., Wyithe J. S. B., 2008, *ApJ*, 672, 1103
Melatos A., Warszawski L., 2009, *ApJ*, 700, 1524
Mendell G., 1991, *ApJ*, 380, 530
Passamonti A., Andersson N., 2009, in preparation
Passamonti A., Haskell B., Andersson N., 2009, *MNRAS*, 396, 951
Peralta C., Melatos A., 2009, *ApJ*, 701, L75
Peralta C., Melatos A., Giacobello M., Ooi A., 2005, *ApJ*, 635, 1224
Peralta C., Melatos A., Giacobello M., Ooi A., 2006, *ApJ*, 644, L53
Prix R., 2004, *Phys. Rev. D*, 69, 043001
Prix R., Comer G. L., Andersson N., 2002, *A&A*, 381, 178
Prix R., Comer G. L., Andersson N., 2004, *MNRAS*, 348, 625
Prix R., Rieutord M., 2002, *A&A*, 393, 949
Ruderman M., 1976, *ApJ*, 203, 213
Shapiro S. L., Teukolsky S. A., 1983, Black holes, white dwarfs, and neutron stars. New York, Wiley-Interscience, 1983
Sidery T. L., 2008, Ph.D. Thesis, Southampton University
Thorne K. S., 1980, Reviews of Modern Physics, 52, 299
van Eysden C. A., Melatos A., 2008, Classical and Quantum Gravity, 25, 225020
Warszawski L., Melatos A., 2008, *MNRAS*, 390, 175
Watts A. L., Strohmayer T. E., 2007, *Ap&SS*, 308, 625
Yoshida S., Eriguchi Y., 2004, *MNRAS*, 347, 575